

Driving Low Frequency Azimuthal Mode in Cylindrical Hall Thruster with a Segmented Anode

IEPC-2013-176

*Presented at the 33rd International Electric Propulsion Conference,
The George Washington University, Washington, D.C., USA
October 6–10, 2013*

Yuan Shi*, Scott Keller, Yevgeny Raitses, and Ahmed Diallo
Princeton Plasma Physics Laboratory, Princeton, New Jersey 08543, USA

Abstract: Coherently rotating $m=1$ azimuthal modes in a cylindrical Hall thruster can be driven using a segmented anode in appropriate thruster regimes. To drive this mode, a square-wave voltage between 225V and 275V is applied to four anode segments with successive 90° phase shifts. A fast camera is used to monitor global fluctuations in the plasma. Planar Langmuir probes and emissive probes are used to obtain time-dependent plasma parameters. At pressures of $\sim 7 \times 10^{-5}$ Torr, driving induces periodic fluctuation of plasma potential, density and temperature, but no coherent $m=1$ mode forms. At pressure $\sim 5 \times 10^{-5}$ Torr, a mode known as “spoke” naturally occurs and rotates in the $\mathbf{E} \times \mathbf{B}$ direction. Driving at the natural spoke frequency in the $\mathbf{E} \times \mathbf{B}$ direction enhances the coherence of the spoke, while driving at other frequencies or in the $-\mathbf{E} \times \mathbf{B}$ direction generally suppresses the spoke.

Nomenclature

B	= brightness
I	= segment current
f	= oscillation frequency
N_e	= electron density
T	= oscillation period
T_e	= electron temperature
V	= segment voltage
V_c	= cold floating potential
V_h	= hot floating potential
V_p	= plasma potential

*Email: yshi@pppl.gov

I. Introduction

Cylindrical Hall thrusters (CHTs) are a modified version of the conventional annular Hall thruster scaled for low power applications (~ 100 W).^{1,2} In particular, the surface area to volume ratio is reduced by eliminating the annular component in the near-exit region of the thruster channel. This change reduces the level of deleterious plasma-surface interactions, such as secondary electron emission, which have the potential to interfere with stable device operation.³

High-speed imaging studies and probe measurements of Hall thruster discharges have revealed the presence of regions with increased density and light emission rotating along the azimuthal $\mathbf{E} \times \mathbf{B}$ direction. These structures, commonly known as spokes, have been ubiquitously observed and are shown to increase cross-field electron transport levels. However, the physical mechanisms underlying these phenomena are insufficiently understood.^{4,5}

Ellison *et al.* developed a segmented anode in order to track and characterize the spoke within the channel of a 2.6 cm CHT. This setup enabled direct measurement of the current traversing each quadrant of the device. Furthermore, centered about each anode, four probe locations were axially aligned to provide density, temperature, and plasma potential measurements for all regions. Results suggested that 50 % of the total current conducted to the anode travelled through the spoke. Temperature and plasma potential variations 135° out of phase with the density perturbations acted to create an induced azimuthal electric field that drives electron transport towards the anode.⁶

Using the same configuration, Griswold *et al.* connected each of the four anode segments to the main thruster power supply using a set of resistors. This correlates to a potential drop that varies proportionally to the spoke-induced increase in current. By such means, the perturbations were suppressed by providing a feedback mechanism to counteract the enhanced transport. The diminished fluctuation levels that result by lowering the anode voltage also suggested that the structure forms through a related ionization instability.⁷

This study considers a reverse configuration in order to characterize these phenomena. In particular, while the boundary conditions along the anode may be fixed in such a way that suppresses the oscillations, amplification may result from driving each segment with a periodic increase in voltage. In this way, the artificially produced and natural perturbations may be compared to probe how the spoke is activated and maintained in various regimes. Furthermore, heightened activity and increased coherence allow for a wider variety of diagnostics to be utilized, such as time resolving laser induced fluorescence (LIF).³ Results will be presented in greater detail in an upcoming journal paper.

This paper is structured as follows: section II provides an overview of the experimental facility and methods used in order to drive and diagnose spoke phenomena. Section III contains experimental results for each operating regime, while conclusions are presented in section IV.

II. Experimental Setup

All experiments were performed at the small Hall thruster facility (SHTF) at the Princeton Plasma Physics Laboratory (PPPL) using the 2.6 cm cylindrical Hall thruster described elsewhere.^{4,6,7} Two operating regimes were considered, corresponding to high and low background pressure levels maintained by the steady-state balance of xenon flow through the thruster and background gas expulsion via a turbo-molecular pumping system. An ionization gauge was used to monitor the pressure levels. Experiments were run using the “direct” magnetic field configuration, in which the radial component of the field lines points inwards, fixing a natural $\mathbf{E} \times \mathbf{B}$ rotation direction with the electric field pointing towards the channel exit. A hollow cathode neutralizer was displaced 57.5 mm radially from the thruster centerline and 20 mm axially from the exit. While the vacuum chamber was maintained at ground, the cathode and thruster bodies were allowed to float. In contrast to past studies, the magnetic field was maintained at half of its nominal value for corresponding front and back coil current levels. Half of the front coil was removed to facilitate the insertion of probes through the channel walls.

High pressure operation ($p \sim 7 \times 10^{-5}$ Torr) was upheld under flows of 4 standard cubic centimeters per minute (SCCM) and 2 SCCM through the anode and cathode, respectively. The magnetic field was optimized such that naturally appearing azimuthal oscillations were most pronounced. The back and front coil currents were set at 2.5 A and 1 A, while the cathode keeper current was upheld at 0.5 A. Furthermore, 12 A of cathode heater current was applied to provide operational stability. In the low pressure regime ($p \sim 5 \times 10^{-5}$ Torr), the flow rates were 3 SCCM and 1.5 SCCM for the anode and cathode, while the back

coil current was adjusted to 2.8 A. All other operating parameters were held constant.

Discharges were studied using natural and artificially driven boundary conditions along the segmented anode. The driving scheme was applied by exposing each consecutive anode segment to 90° phase-shifted square wave voltages varying between 225 V and 275 V:

$$V_i(t) = 225 + 50S(t + (i - 1)T/4) \quad (1)$$

where the subscript i denotes the i th segment, and the function $S(t)$ at time t is defined using the driving period $T = 1/f$ such that:

$$S(t - nT) = \begin{cases} 1, & (t - nT)/T < 0.5 \\ 0, & 0.5 < (t - nT)/T < 1 \end{cases} \quad (2)$$

for any integer value n . In the natural regime, a constant applied discharge voltage of 250 V was considered. The phase-shifted driving voltages are constructed using a logic circuit that functions using a 4f master clock signal output of a function generator to control a series of transistors connecting each segment to either the 225 V or 275 V voltage source. Individual segment currents were obtained by measuring the voltage drop across a set of resistors using differential amplifiers. Therefore, accuracy is limited to the extent that the resistances are known. The applied driving frequency was varied between ± 30 kHz for high pressure operation and ± 16 kHz for low pressure operation in order to track the induced plasma response, and the degree of coherence of rotating structures. (The negative frequencies denote driving in the $-\mathbf{E} \times \mathbf{B}$ direction.) Frequency ranges were chosen in order to probe about the natural oscillation frequencies of 12 kHz and 6 kHz for high and low background pressure conditions, respectively.

A Phantom v7.3 digital camera was used to visually record the axially integrated light emission intensity profile at each angular and radial location of the thruster channel. The camera was mounted outside of the vacuum chamber and optically aligned with the plume exit using a set of mirrors. The images were captured at a rate of 142,857 fps and digital resolution of 64×64 pixels. The integrated pixel intensity across each quadrant was used in post-processing to determine the phase-shifted correlation in brightness between consecutive segments.

A set of Langmuir probes were installed in the near-anode region of the thruster to determine the ion saturation current in each domain and relate that to the time-varying density profile. This placement scheme particularly provides measurements within the ionization region of the thruster. Probe tips were placed flush with the channel surface in order to minimize any perturbations of the plasma. Each probe consisted of a single bored alumina tube with outer and inner diameters of 0.045 in and 0.75 mm, respectively. Emissive probes were used to acquire the electron temperature (T_e) and plasma potential (V_p). The relation between these quantities with the hot (V_h) and cold (V_c) floating potentials was assumed to be:⁶

$$V_h = V_p - 2T_e \quad (3a)$$

$$V_c \sim V_p - 5.77T_e \quad (3b)$$

Each emissive probe was constructed using a double bored alumina tube with a 0.125 mm diameter thoriated tungsten filament wire packed with six tungsten filler wires in each hole. The probes were placed such that the filament was ejected into the plasma with the ceramic tube slightly below the surface. Furthermore, plume measurements of the ejected xenon ions were obtained using a rotating, electrostatic probe (1.1 cm in diameter) with a guarding sleeve, in conjunction with a back-facing probe, which was used to subtract background current levels. Each probe was biased at -30 V in order to reach the ion saturation regime, in which electrons are repelled, thereby providing a measure of the total ion current ejected from the device. The radial distance to the plume probes from the thruster exit is 15 cm. A motor was used in conjunction with a data acquisition system to determine the ion fluxes at each angular location around the exit as the probe system rotates. The resulting current and propellant utilization efficiencies were calculated in conjunction with the degree of plume divergence for each setting. Integration of the measured current density was performed along a half-sphere subtending the channel exit while assuming azimuthal symmetry.⁸

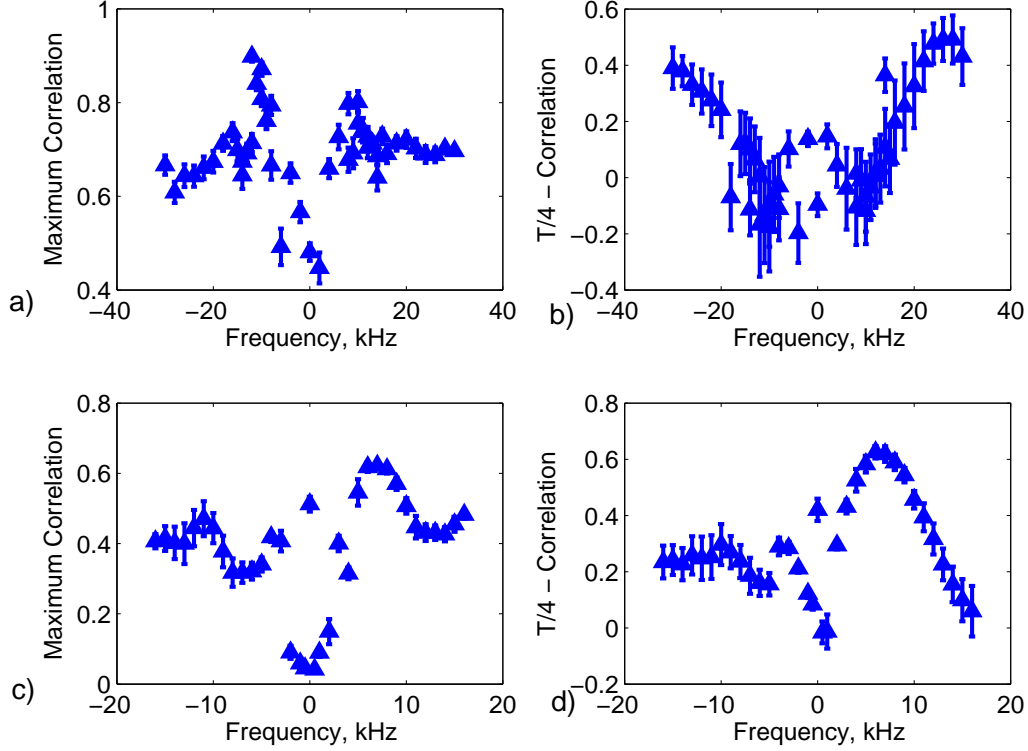


Figure 1. The maximum statistical correlation in segment brightness for arbitrary and quarter-period phase shifts for the high (a and b) and low (c and d) pressure regimes across various driving frequencies.

III. Experimental results

The main criterion used to distinguish spoke oscillations from incoherent fluctuations is the cross-correlation. In particular, oscillations that exhibit high degrees of coherence (~ 0.5 or greater) between brightness data across consecutive segments are considered. The phase shift in time domain must be near a quarter period to reflect a rotating structure. The data presented in Figure 1 show that only the low pressure case exhibits a naturally rotating (driving frequency of 0 kHz) mode. The natural frequency was calculated near 6 kHz using camera measurements. Furthermore, the quarter-period phase-lag correlation at this equivalent driving frequency exhibits the maximum value of 0.63 for low pressure operation. While driving amplifies and confines activity when rotating in the positive direction (along $\mathbf{E} \times \mathbf{B}$), the same degree of order is not observed when driving in the opposite direction. The case of high pressure exhibits several differences. While there are no naturally coherent rotations, the degree of quarter-phase shifted coherence increases significantly at higher driving frequencies. However, Figure 2 presents the level of phase shifting needed to achieve the maximal level of time-lagged correlation, and the condition for uniform rotation is satisfied only when driving near the naturally occurring rotation frequency (~ 6 kHz) under low pressure background conditions. Changes in background pressure on thruster operation have also been shown to affect naturally occurring spoke activity in previous studies.⁹

The traces presented in Figure 3, which are obtained by averaging over ~ 1000 oscillations, show that the plasma potential and electron temperature generally respond in phase with the modulation of the corresponding anode segment voltage for both driving cases considered. 12 kHz was chosen as the driving frequency with the highest correlation between the currents through consecutive segments. However, when driving in the negative direction, the segment current is roughly 180° out of phase with the applied voltage. Furthermore, the current reaches a sharp peak in the case of positive driving while the voltage remains at a maximum for a prolonged duration.

Driving at low pressure, as shown in Figure 4, contrasts with the high pressure case as manifested through

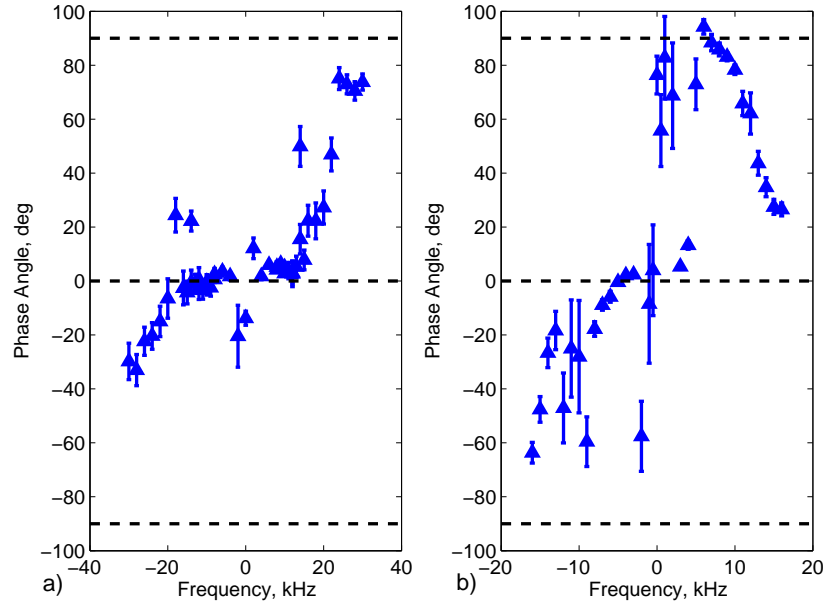


Figure 2. The phase angle needed to achieve maximum correlation in the time-varying brightness series across consecutive segments. (a) High and (b) low pressure cases are presented. The dashed lines are used to signify the phase shift characteristics of uniform azimuthal rotation ($\pm 90^\circ$) and no rotation (0°).

the phase relationships between the variable quantities. In particular, the measured brightness, current and density vary closely in phase with the voltage modulation and temperature variations. Similar oscillations are observed while driving along and against the $\mathbf{E} \times \mathbf{B}$ drift direction. Results suggest that the coupled effects of reduced flow rate and background density have profound implications on the activity of rotating modes. Driving with square-wave, as opposed to sinusoidal, voltages may also contribute to such behavior. Small scale fluctuations in the traces shown in Figure 3 and 4 suggest that high frequency activity may also be prevalent within the global evolution of the plasma.

The results of plume measurements exhibited in Figure 5 show that driving spoke activity has negligible effects on the characteristics of the plume, even at the resonance driving condition under low pressure. This suggests that the resulting perturbations do not affect the propagation of ions as they are accelerated out of the thruster channel. One possibility is that the ionization induced instability directly affects only the plasma in the near-anode region. As a result, the performance characteristics of the device remain unchanged in each operating regime.

IV. Conclusions

The principle that plasma oscillations may be induced through the appropriate tuning of boundary conditions along a segmented anode has been shown. Background and facility effects are also found to couple with thruster operation. While the fundamental mechanisms of this coupling are beyond the scope of this report, it is noteworthy that small variations ($\sim 10^{-5}$ Torr) in background pressure can induce large changes in the resulting coherence properties. Probe measurements show that while the plasma parameters undergo cyclic variation in the near-anode region, the plume response remains unaffected. These results suggest that further study needs to be performed in order to determine how the driven spoke affects the phase space distribution of particles throughout the thruster channel. Advanced diagnostic techniques such as laser induced fluorescence may provide insight into the dynamics of the potential instabilities that induce spoke activity. Detailed interpretation of driven spoke activity compared to a naturally occurring spoke will appear in an upcoming journal article.

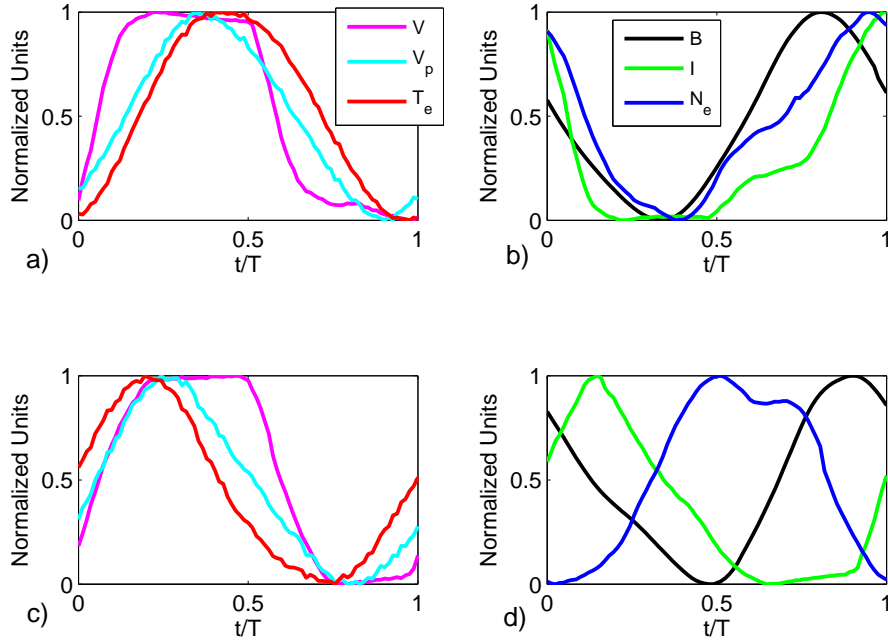


Figure 3. Normalized traces of segment oscillations over an oscillation period at high pressure. Values are synchronized and averaged between all four anode segments. Driving is performed at 12 kHz in the negative (a and b) and positive (c and d) directions. The segment current has a maximum of 1.86 (1.22) A, density a maximum of 2.06×10^{12} (2.13×10^{12}) cm^{-3} , temperature a maximum of 42.35 (44.66) eV, and plasma potential a maximum of 257.6 (272.5) V in the near-anode region for reverse (forward) driving. The segment current has a minimum of -0.05 (-0.08) A, density a minimum of 1.77×10^{12} (1.87×10^{12}) cm^{-3} , temperature a minimum of 39.73 (42.82) eV, and plasma potential a minimum of 248.6 (265.4) V in the near-anode region for reverse (forward) driving.

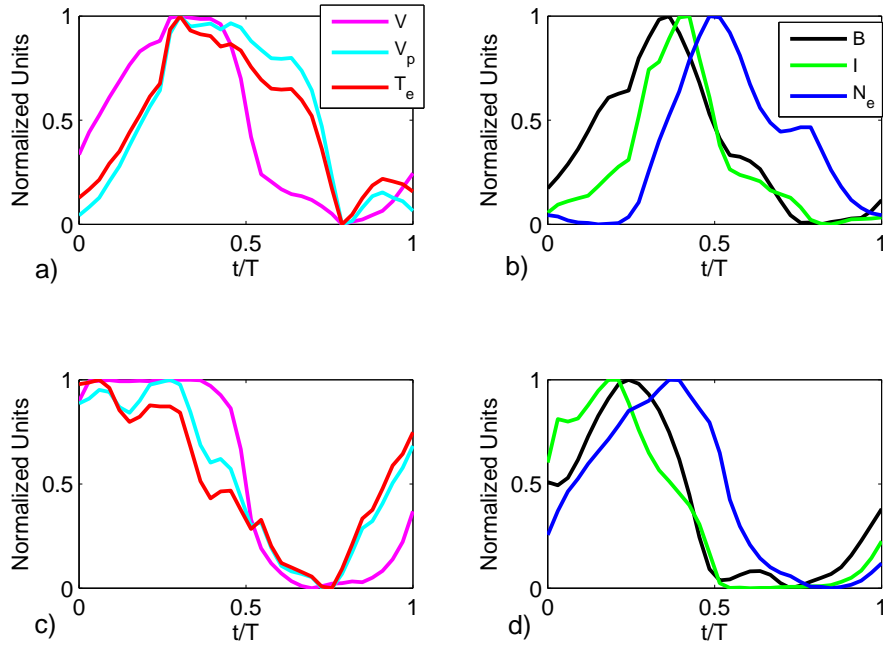


Figure 4. Normalized traces of plasma parameters at low pressure. Driving at 6 kHz is performed in the negative (a and b) and positive (c and d) directions. The segment current has a maximum of 1.19 (0.44) mA, density a maximum of 2.44×10^{12} (3.49×10^{12}) cm^{-3} , temperature a maximum of 11.09 (7.55) eV, and plasma potential a maximum of 250.3 (243.3) V in the near-anode region for reverse (forward) driving. The segment current has a minimum of 0.01 (0.0) A, density a minimum of 0.79×10^{12} (1.01×10^{12}) cm^{-3} , temperature a minimum of 5.27 (3.88) eV, and plasma potential a minimum of 217.0 (219.8) V in the near-anode region for reverse (forward) driving.

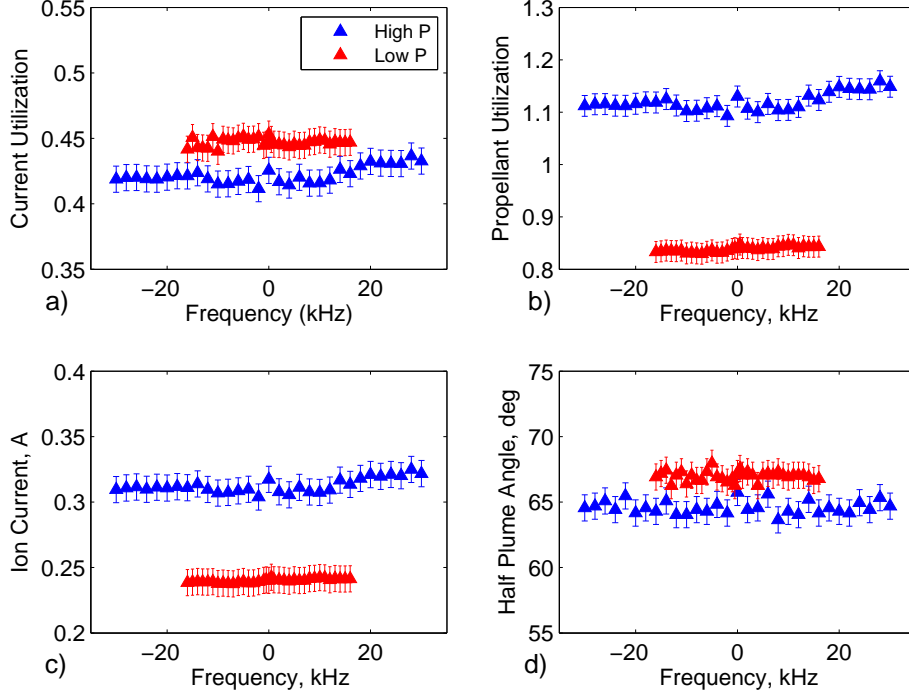


Figure 5. The current (a) and propellant (b) utilization efficiencies along with the total ion current (c) and plume divergence (d) calculated from plume probe measurements at each driving frequency for each background pressure considered.

V. Acknowledgments

This work was partially supported by AFOSR. We thank Dr. Stephane Mazouffre for fruitful discussion. We thank Lee Ellison for help with experiments and Alexandre Merzhevskiy for expertise on electronics.

VI. References

- ¹Raitses, Y., and Fisch, N. J., “Parametric Investigations of a nonconventional Hall thruster,” *Physics of Plasmas*, Vol. 8, 2579, 2001.
- ²Smirnov, A., Raitses, Y., and Fisch, N. J., “Experimental and theoretical studies of cylindrical Hall thrusters,” *Physics of Plasmas*, Vol. 14, 057106, 2007.
- ³Spektor, R., Diamant, K. D., Beiting, E. J., Raitses, Y., and Fisch, N. J., “Laser induced fluorescence measurements of the cylindrical Hall thruster plume,” *Physics of Plasmas*, Vol. 17, 093502, 2010.
- ⁴Parker, J. B., Raitses, Y., and Fisch, N. J., “Transition in electron transport in a cylindrical Hall thruster,” *Applied Physics Letters*, Vol. 18, 091501, 2010.
- ⁵McDonald, M. S., and Gallimore, A. D., “Rotating Spoke Instabilities in Hall Thrusters,” *IEEE Transactions on Plasma Science*, Vol. 39, No. 11, 2011.
- ⁶Ellison, C. L., Raitses, Y., and Fisch, N. J., “Cross-field electron transport induced by a rotating spoke in a cylindrical Hall thruster,” *Physics of Plasmas*, Vol. 19, 013503, 2012.
- ⁷Griswold, M. E., Ellison, C. L., Raitses, Y., and Fisch, N. J., “Feedback control of an azimuthal oscillation in the $E \times B$ discharge of Hall thrusters,” *Physics of Plasmas*, Vol. 19, 053506, 2012.
- ⁸Smirnov, A., “Experimental and Theoretical Studies of Cylindrical Hall Thrusters,” Ph.D. Dissertation, Dept. of Astrophysical Sciences, Princeton Univ., Princeton, NJ, 2006.
- ⁹Raitses, Y., Parker, J. B., Davis, E., and Fisch, N. J., “Background Gas Pressure Effects in the Cylindrical Hall Thruster,” *AIAA*, 6775, 2010.